



Article

Annotation of the 12th Chromosome of the Forest Pathogen *Fusarium circinatum*

Tadeusz Malewski ¹, Slavica Matić ², Adam Okorski ³, Piotr Borowik ⁴ and Tomasz Oszako ^{5,*}¹ Museum and Institute of Zoology, Polish Academy of Science, ul. Wilcza 64, 00-679 Warszawa, Poland² Institute for Sustainable Plant Protection (IPSP), National Research Council of Italy (CNR), Strada delle Cacce 73, 10135 Torino, Italy³ Department of Entomology, Phytopathology and Molecular Diagnostics, Faculty of Agriculture and Forestry, University of Warmia and Mazury in Olsztyn, Pl. Łódzki 5, 10-727 Olsztyn, Poland⁴ Faculty of Physics, Warsaw University of Technology, ul. Koszykowa 75, 00-662 Warszawa, Poland⁵ Department of Forest Protection, Forest Research Institute, ul. Braci Leśnej 3, 05-090 Sękocin Stary, Poland

* Correspondence: T.oszako@ibles.waw.pl

Abstract: The genus *Fusarium* comprises more than 300 species, and many of them are pathogens that cause severe diseases in agricultural, horticultural and forestry plants in both anthropogenic and natural ecosystems. Because of their importance as plant pathogens, the genomes of several *Fusarium* spp. have been sequenced. Within this genus, *Fusarium circinatum* is one of the most harmful pathogens of pine trees attacking up to 60 *Pinus* species. Till now, the genomes of 13 strains of *F. circinatum* have been sequenced. The strain GL1327 we studied lacks a twelfth chromosome, which allows the study of virulence genes on this chromosome. Although the genome of several strains of *F. circinatum* has been sequenced, it is still almost completely unannotated, which severely limits the possibilities to further investigate the molecular mechanisms of virulence of *Fusarium*. Therefore, this study aimed to annotate the 12th chromosome of *F. circinatum* and integrate currently available resources. In silico annotation of the 12th chromosome of *F. circinatum* revealed the presence of 118 open reading frames (ORFs) encoding 141 proteins which were predicted using an ab initio gene prediction tool. The InterProScan and SMART analyses identified known domains in 30 proteins and eggNOG additionally in 12 of them. Among them, four groups can be distinguished: genes possibly related to heterokaryon incompatibility (4 genes), regulation of transcription (5 genes), plant cell wall degrading enzymes (7 genes) and trichothecene synthesis (3 genes). This study also integrated data of *F. circinatum* reference strain CMWF1803 assembled to chromosome level but not annotated with currently best annotated but assembled only to scaffold level strain NRRL 25331.



Citation: Malewski, T.; Matić, S.; Okorski, A.; Borowik, P.; Oszako, T. Annotation of the 12th Chromosome of the Forest Pathogen *Fusarium circinatum*. *Agronomy* **2023**, *13*, 773. <https://doi.org/10.3390/agronomy13030773>

Academic Editor: Pedro Talhinhas

Received: 10 February 2023

Revised: 1 March 2023

Accepted: 6 March 2023

Published: 7 March 2023



Copyright: © 2023 by the authors. Licensee MDPI, Basel, Switzerland. This article is an open access article distributed under the terms and conditions of the Creative Commons Attribution (CC BY) license ([https://creativecommons.org/licenses/by/4.0/](https://creativecommons.org/licenses/by/)).

1. Introduction

Fusarium is a cosmopolitan genus of filamentous ascomycetes (Sordariomycetes: Hypocreales: Nectriaceae) that includes many toxin-producing plant pathogens of agricultural importance. The genus *Fusarium* includes over 300 phylogenetically distinct species [1]. Many of these species are plant pathogens that cause serious diseases on agricultural, horticultural and forestry plants in anthropogenic and natural ecosystems [2].

Pine Pitch Canker Disease (PPC), a serious threat that attacks many pine species, is caused by the pathogenic fungus *Fusarium circinatum* Nirenberg & O'Donnell (teleomorph = *Gibberella circinata*). *F. circinatum* belongs to the EPPO A2 quarantine pathogen and causes one of the most devastating diseases in pine forests, afforestations and nurseries, not only in Europe but throughout the world [3]. The host range of *F. circinatum* is very broad and includes up to 60 *Pinus* species [4,5].

Although the whole genome sequence of about 44 Mb of *F. circinatum* has been determined [6], our knowledge of the fungal genes involved in its pathogenic behaviour is limited. Seven putative quantitative trait loci associated with mycelial growth and colony

margins have been described [7]. Van Wyk et al. [8] discovered a locus that possibly determines the growth rate near the telomere of chromosome 3. The sequence of this locus is highly conserved in *F. circinatum* and its close relatives, except for a 12,000 bp insertion encoding five genes. An *in silico* analysis of the *F. circinatum* genome identified five candidate genes related to the growth (*Fcfga1*, *Fcfgb1*, *Fcac*, *Fcrho1*, and *FcpacC*) [9]. Functional studies of *Fcrho1* deletion mutants, a Rho-type GTPase, showed significantly reduced growth *in vitro* than the corresponding ectopic and wild-type strains. The knockout mutant of *Ras2*, another gene encoding the GTPase, also produced significantly smaller lesions compared to the complementation mutants and wild-type strains. Growth studies showed also significantly smaller colonies and delayed germination of conidia in the knockout mutant strain [10].

Currently, the genomes of 13 strains of *F. circinatum* have been sequenced [11], providing a solid basis for comparative genomics. One of them (GL 1327) lacks a 12th chromosome [12], which provides favourable conditions for the identification and study of genes determining the virulence of *F. circinatum*.

The aim of this study was to identify ORFs localised on the 12th chromosome and subsequently characterise the encoded proteins.

2. Materials and Methods

Analysis In Silico

The sequence of the 12th chromosome (Assembly ASM2404739v1, Acc. No. CM043929.1) from the representative genome of *F. circinatum* Mexican strain CMWF1803 from *Pinus patula* [11] was retrieved from NCBI. Gene prediction was performed with the programme AUGUSTUS version 3.3.1 trained for *F. graminearum* with the ab initio gene prediction method [13,14].

The predicted protein sequences were analysed against the protein database NCBI-NR using BLASTp (default identity $\geq 40\%$, coverage $\geq 40\%$). Functional analysis of predicted protein sequences was performed using InterProScan 91.0 [15,16] against the integrated InterPro database consisting of PRINTS, SMART, Pfam, SUPERFAMILY, CATH -Gene3D, PANTHER and CDD databases [17], Simple Modular Architecture Research Tool (SMART v.9) [18] and against the unsupervised orthologous group database EggNOG v6.0 [19].

3. Results

In Silico Characterisation of Putative *F. circinatum* Genes

The sequence of the 12th chromosome was processed for ab initio gene prediction using AUGUSTUS. A total of 118 putative genes were predicted, of which 56 are located on the plus strand and 62 on the minus strand (Table A1 in Appendix A). These genes can be transcribed into 141 transcripts. Thirty-six transcripts were intronless, while 41, 28, 10, 8, 7, 3, 2 and 1 transcripts have one, two, three, four, five, seven, either six or eight, and nine introns, respectively.

Six genes (*g1*, *g19*, *g20*, *g31*, *g56* and *g76*) had two alternative transcription start sites, and the transcripts of 21 genes had no alternative splicing. The putative genes correspond to five scaffolds of *F. circinatum* strain NRRL 25331 (PRJNA565749): JAAQPE010000042.1-142267 bp; JAAQPE010000057.1-51020 bp; JAAQPE010000172.1-29236 bp; and JAAQPE010000262.1-90105 bp (Figure 1). The identity of the four scaffolds to the CM043929 sequence ranged from 99.09% to 99.81%, with only scaffold JAAQPE010000057.1 having 93.44%.

The predicted protein sequences were compared with sequences deposited in GenBank using BLASTp. Out of 141 queries, 130 sequences were highly identical (>90%) to *F. circinatum* strain NRRL 25331, seven proteins had lower identity (*g99t2*, 76.34%; *g115t1*, 81.17%; *g16t1*, 81.33%; *G99t1*, 84.22%; *G92t2*, 86.52%; *G87t2*, 87.94%; *g78t1*, 87.97%) and four (*g48t1*; *g59t1*; *g74t1*; *G98t1*) were not identical to *F. circinatum* but identical to other *Fusarium* species.

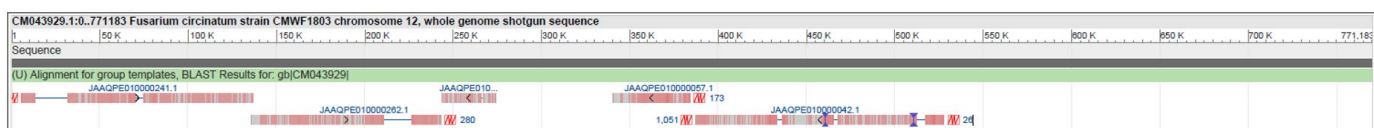


Figure 1. Localization of the scaffolds of *F. circinatum* strain NRRL 25331 on the 12th chromosome of the representative genome of *Fusarium circinatum* strain CMWF1803. Black bar—reference sequence of *F. circinatum* 12th chromosome CMWF1803 strain with coordinates of the sequence. Blue letters—names of *F. circinatum* strain NRRL 25331 scaffolds. Grey/red boxes—scaffolds of *F. circinatum* strain NRRL 25331. Insertions are marked with blue two hourglass-like triangles.

With the help of InterProScan and SMART, domains and protein architectures could be identified for 30 proteins (Table A3 in Appendix A). Among them, four groups can be distinguished: Genes possibly related to heterokaryon incompatibility, regulation of transcription, plant cell wall degrading enzymes and trichothecene synthesis.

Among the genes predicted by Augustus, four genes were found to be related to heterokaryon incompatibility (Figure 2). The protein g57t1 has two domains: Heterokaryon incompatibility (HET) and protein kinases (S-TKc). This protein sequence is identical to KAF5666823.1 (100% search coverage, 100% identity) of *F. circinatum* strain NRRL 25331, but is only referred to as serine-threonine kinase in GenBank. Four proteins (g26t1, g52t1 and g58t1 and g58t2) contain a NACHT nucleoside triphosphatase domain (named after the NAIP, CIITA, HET-E and TP-1 proteins) flanked by a varying number of ankyrin repeat domains. The alternative splicing of the g58 transcript has no effect on the protein architecture. In the g26t1 and g52t1 proteins, the nucleoside phosphorylase domain (PNP-UDP-1) is located proximal to NACHT; in addition, g52 contains the domain oxoglutarate/iron-dependent dioxygenase (2OG-FeII-Oxy).

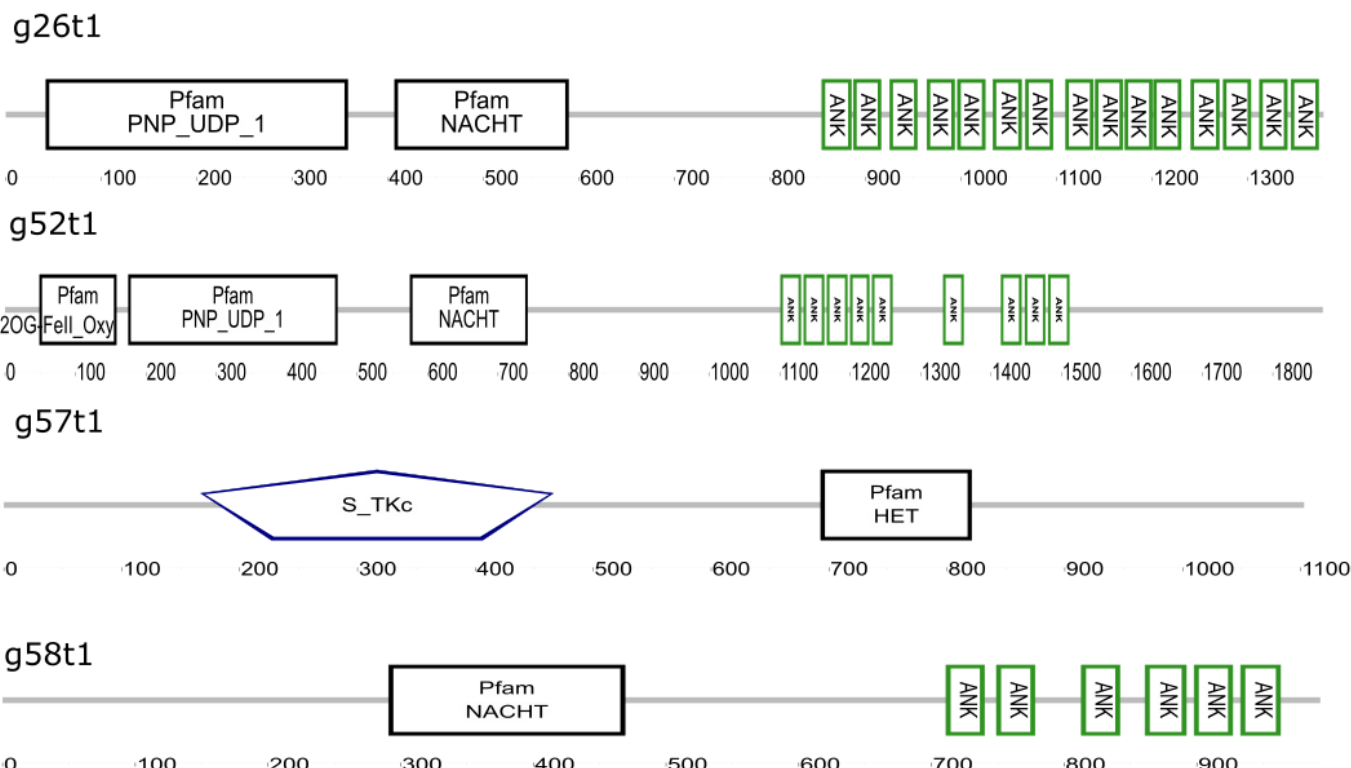


Figure 2. Architecture of proteins potentially involved in heterokaryon incompatibility. Black rectangles—protein domains related to heterokaryon incompatibility. Green rectangles—ankyrin domain repeats. Blue polygon—protein kinases domain.

The incompatibility reaction is associated with massive transcriptional reprogramming. Four genes (*g20*, *g55*, *g82* and *g83*) encoding putative transcription factors were found on the 12th chromosome. The protein *g20t1* contains a Jumonji domain (JmjC). *G82* contains a transcription factor domain specific for fungi (Fungal-trans). This protein sequence is identical to KAF5673552.1 (100% search coverage, 100% identity) of *F. circinatum* strain NRRL 25331, where it is designated cutinase transcription factor 1 alpha. The *G55* transcript is subject to alternative splicing, but this does not affect the protein architecture. Both proteins (*g55t1* and *g55t2*) have two domains: Fungal-trans and GAL4. The *G83* protein (Table A4 in Appendix A) has a fungal binuclear Zn(2)-Cys(6) domain. In addition to the putative transcription factors, the *g103t1* protein contains a SET domain typical of proteins involved in epigenetic regulation of gene expression.

During infection, *Fusarium* secretes various virulence factors, including effector proteins and plant cell wall degrading enzymes (CDWEs). The proteins encoded by *g7* and *g102* contain a lipase GDSL-2 domain. This domain is typical of SGNH hydrolase-type esterases that act as esterases and lipases. The carboxylesterase domain (COesterase) contains the proteins *g81t1* and *g82t2*. Another type of hydrolases-peptidases-encode the genes *g18* and *g89*. The protein *g18t1* contains peptidase C1A, *g98t1* and *g89t2* peptidase C14 or caspase domain. In addition to hydrolases, there are two genes (*g66* and *g105*) on the 12th chromosome that encode proteins containing a domain of the Major Facilitator Superfamily (MSF1).

One of the features of *Fusarium* is toxin synthesis. Three putative genes for trichothecene synthesis have been detected. *G6t1* and *g6t2* contain tyrosinase, *g95t1-p450* and *g70t1*-three acyl-CoA domains. In addition to groups of putative genes related to heterokaryon incompatibility, transcriptional regulation, plant cell wall degrading enzymes and trichothecene synthesis, 13 proteins were found whose products may be involved in many metabolic processes of *Fusarium* metabolic processes. Another 12 proteins were annotated with eggNOG (Table A4 in Appendix A).

4. Discussion

4.1. Distribution of *F. circinatum*, the Causative Agent of PPC Disease

As mentioned in the introduction, the fungal pathogen *F. circinatum* is the causative agent of PPC disease [20]. Does the presence of the 12th chromosome cause the pathogen to severely attack a variety of pine species in forests and nurseries worldwide? The fungus can damage seedlings in nurseries and mature trees in forests. Symptoms in seedlings include wilting and in mature trees bleeding, resinous cankers on trunks or thick branches and tree death [20]. As *F. circinatum* has already been detected in Europe, it is considered a serious, potentially invasive forest pathogen that spreads via infected seeds, seedlings, wood, soil, wind, insect vectors and human activities. In Europe, the fungus has affected pine trees in northern Spain and Portugal and has also been detected in France and Italy. Research on the fungus (including its chromosomes) can therefore contribute to the understanding of its pathogenesis and thus to the development of an appropriate protection strategy. This should apply to young seedlings as well as to adult trees. Despite the economic importance of PPC disease, the worldwide distribution of the pathogen *F. circinatum* is poorly documented and the pathogenicity of its strains is even less known. It is likely that the genetic diversity and population structure of the pathogen influence the spread of PPC, including in Europe (models for the likely spread of the disease), and the susceptibility of hosts. Chromosome number could be important for the virulence of *F. circinatum*, which also depends on host species, tree age and environmental characteristics. Knowledge of the above factors is crucial for disease management, containment and mitigation strategies. The in silico analyses carried out should help countries that are currently free of *F. circinatum* to put in place effective procedures and restrictions and prevent the invasion of the pathogen.

4.2. Development of New Diagnostic Methods to Ensure Reduction of PPC

Fusarium circinatum is on the list of species recommended for regulation as a quarantine pest in Europe. More than 60 species of *Pinus* are susceptible to this pathogen, and it also attacks Douglas-fir (*Pseudotsuga menziesii* (Mirb.) Franco) and species from genera such as *Picea* and *Larix*. The European Food Safety Authority (EFSA) estimates the probability of reintroduction into the EU as very high [21]. Thanks to the possibility of early detection, continuous surveillance and inspections by quarantine services, outbreaks of *F. circinatum* in Italy and France have been officially eradicated. However, the global spread of *F. circinatum* suggests that the pathogen will continue to be found in new areas in the future. Rapid identification of the most virulent strains of the pathogen (using knowledge of their chromosomes) will be important in Europe and elsewhere to limit the spread of the disease. Currently, morphological identification methods are being replaced by molecular methods, which include conventional PCR with a specific target region in the intergenic interval and various real-time PCR protocols with varying specificity and sensitivity [22]. Perhaps the search for chromosome 12 will also be useful for pest risk assessment.

4.3. Pathways of Transmission and Potential Host Risk of the Pathogen

As *F. circinatum* is the causal agent of one of the most devastating forest diseases worldwide, its spread over long distances should be controlled, especially by monitoring infected seeds. On the other hand, at the regional level, seedlings, substrates and containers play an important role in the spread of the fungus [21]. The pathogen enters nurseries via infected seeds and is further spread by planting infected plants, especially since infected plants (asymptomatic) may appear without disease symptoms. Once established, *F. circinatum* is spread by rain, wind and insects. Natural spread of the pathogen is limited due to the short spore dispersal distances and the relatively short flight distances of the spreading insects. To understand how best to intervene in the development of the disease in nurseries and forests, we conducted annotation of twelfth chromosome.

4.4. Risk of Establishing the Pathogen in New Regions in Europe

Pine trees as potential host plants are important components of native forests and plantations in Europe, where they play an important role both economically and ecologically. Pine diseases are mainly caused by fungal pathogens and can significantly affect the survival, vigour and yield of both individual trees and entire stands or plantations. PPC caused by *F. circinatum*, one of the most devastating pine diseases in the world, is an example of a new invasive disease in Europe.

The susceptibility of Scots pines in Poland (*Pinus sylvestris* L.) to infection by *F. circinatum* was tested in a greenhouse trial by [23]. Sixteen Polish pine cultivars were artificially inoculated with the 12th chromosome of *F. circinatum* and six other *Fusarium* species known to infect pine seedlings in nurseries. All pines were found to be highly susceptible to PPC and showed varying degrees of susceptibility to the other *Fusarium* species tested. The results suggest that the risk of establishment of the invasive pathogen *F. circinatum* may be high as a result of its accidental introduction in Poland.

In the future, the fungus is more likely to spread in the pine forests of southern Europe, but there is also the possibility of spread in central and northern Europe. In Lithuania, no occurrence of *F. circinatum* has been reported so far. In 2018, the susceptibility of three different native Lithuanian *Pinus sylvestris* provenances to this pathogen [24] was tested. For each origin, 38 pines were used and the soil was inoculated with a suspension of *F. circinatum*, and DNA was extracted from several plants that appeared unhealthy four weeks after soil inoculation. Using the real-time PCR method, *F. circinatum* could not be detected in these samples. However, the reason could be that the fungal biomass was too low in relation to the host biomass or that the strain was less pathogenic than others.

4.5. Possible Interactions between *F. circinatum* and Other Fungal Species

The impact of microbiome interactions on plant health and the possible role of the plant microbiome in disease expression have been the subject of several recent studies [24]. In Lithuania, the interaction between 12th chromosome strain of *F. circinatum* and several pine-inhabiting fungi such as *Dothistroma septosporum*, *F. oxysporum* and *Lecanosticta acicola* was also verified [24]. It was found that *F. oxysporum* grows slightly faster than *F. circinatum* and inhibits the growth rate of *F. circinatum*. *D. septosporum* produced dothistromin, which also appeared to slow the growth of the *F. circinatum* culture. In the meantime, *L. acicola* was displaced by *F. circinatum*.

Co-infection of trees with indigenous pathogenic fungi or alien oomycetes and *F. circinatum* is possible. Biotic interactions could play an important role in the establishment of the PPC pathogen in European nurseries and forests [25]. Available information on pine pathogens that may co-occur with *F. circinatum* in Europe will have an impact on pine survival and growth. Early and accurate identification of *F. circinatum*, a recently introduced pathogen currently being regulated in Europe, is crucial to prevent its introduction and spread in forests. Chromosome studies could provide valuable information in this regard if it is confirmed that the high pathogenicity of some strains of the fungus depends on them and others do not.

4.6. In Silico Approach to the Identification and Characterisation of Genes

In this study, we used a genome-based in silico approach to identify and characterise genes located on the 12th chromosome of *F. circinatum*. Chromosome 12 has been shown to be the smallest of the chromosomes found in species of the *F. fujikuroi* complex. The size of these chromosomes varies considerably intra- and interspecifically and shows polymorphism in chromosome length compared to the other chromosomes [26].

Fungal cells can interact with each other either vegetatively or sexually. In ascomycete fungi, sexual interactions are controlled by the alleles at the mating type locus (MAT) and asexual interactions by the alleles at the loci *vic* (vegetative incompatibility) or *het* (heterokaryon incompatibility) [27]. In members of the *F. fujikuroi* species complex, 8 to 10 *vic* loci have been identified [28]. Vegetative incompatibility leads to programmed cell death. For programmed cell death associated with vegetative incompatibility, there are important proteins containing HET [29] and NACHT [30] domains. In *F. circinatum* we have found four putative proteins that contain a central NACHT domain. Two of them have an N-terminal PNP-UDP effector domain and all three have a C-terminal ANK repeat domain (Figure 2). This organisation is typical of Ascomycota, where 20% of proteins with NACHT domains have N-terminal PNP-UDP and 42% have C-terminal ANK repeats [30]. Proteins containing the NACHT domain are involved in a process of non-self-recognition and programmed cell death of fungi called heterokaryon incompatibility [31,32].

The incompatibility response has been found to be associated with massive transcriptional reprogramming [33]. Transcription factors (TFs) play a key role in regulating gene expression by binding to DNA in a sequence-specific manner. TFs are usually classified according to their DNA-binding motif. Representatives of 80 TF families are typically found in fungal genomes. The largest of these is the zinc cluster (C6 zinc finger) family [34]. They play an important role in growth, development and pathogenicity [35–37]. Fusarium transcription factor 1 (FTF1) has been described as a potential regulator of effector expression in *F. oxysporum* f. sp. *phaseoli* and *F. oxysporum* f. sp. *lycopersici* [38]. Mahanty et al. [39] described that specialised C6-type TFs may act as major regulators of *F. oxysporum* f. sp. *cepae* pathogenicity during the development of *Fusarium* basal rot in onions.

Proteins with a zinc finger domain were found in the g24t1, g55t1 and g55t2 proteins. SMART identified a transcription factor specific to fungi in the g82t1 domain, while BLAST found sequence identity with KAF5673552.1, which was annotated as cutinase transcription factor 1 (CTF1). CTF1 belongs to the C6 zinc TFs. CTF regulates the expression of cutinases and fatty acid metabolism genes in *F. solani* f. sp. *pisi* [40] and *Aspergillus nidulans* [41]. Disruption of Ctf1α eliminated the phytopathogenicity of *F. solani* [40]. *F. oxysporum* strains

lacking a functional copy of the CTF1 gene are impaired in the induction of cutinase activity and in the expression of genes encoding cutinase and lipase [42].

Gene expression also depends on the methylation of histones. Acetylation of lysine (K) residues in histone 3 (H3) is associated with active transcription, while methylation of lysine or arginine (R) residues leads to a more complex outcome that depends on associated reader proteins [43]. H3K4 and H3K36 are considered to be hallmarks of euchromatin in yeast and higher eukaryotes [44]. In filamentous fungi, the picture appears to be more diverse, as data showed the ubiquitous presence of the H3K36 trimethylation mark (me3) in *F. fujikuroi* and *F. graminearum* [45,46]. Methylation of H3K4 has been shown to depend on the conserved SET domain-containing methyltransferase Set1 [47,48]. While Set1 is responsible for H3K4 methylation in the fungus, jumonji C is responsible for demethylation [49]. On Chr12 of *F. circinatum* we have discovered putative genes encoding both of these proteins: G103t1 contains the SET domain and g20t1 jumonji.

During the infection process, *Fusarium* uses a number of secretion systems and releases a variety of virulence factors such as mycotoxins, effector proteins and CWDEs to overcome the target host cells. CWDEs such as polygalacturonases, pectate lyases, xylanases, peptidases, peptide hydrolases, ribonucleases and cutinases may contribute to pathogenesis by degrading waxes, cuticles and cell walls to promote tissue invasion and pathogen spread [50,51]. Cutinases and lipases that catalyse the hydrolysis of ester bonds from fatty acid polymers, facilitating fungal invasion through the cuticle. Disruption of the lipase gene *FGL1* in *F. graminearum* resulted in reduced extracellular lipolytic activity in culture and reduced virulence in both wheat and maize [52]. Disruption of another lipase gene, *FgATG15*, also greatly attenuated wheat head infection [53]. An active role of lipases in establishing full virulence has also recently been suggested for the plant pathogen *F. oxysporum* f. sp. *lycopersici*, where reduced lipolytic activity due to deletion of lipase regulatory genes resulted in reduced colonisation of tomato plants [54].

The secreted metalloprotease FoMep1 and the serine protease FoSep1 of *F. oxysporum* are involved in full virulence against tomato because they can reduce the antifungal activity of their host plant chitinases [55]. The *FoAYP1* gene also encodes protease. Surprisingly, this protease is secreted by *F. oxysporum* but is localised in the nucleus in plant cells. The knock-out strain of the *FoAYP1* gene showed reduced virulence against tomato plants, but its mycelial growth and conidiation were unchanged [56]. The Major Facilitator Superfamily (MFS) is one of the largest known membrane transporter families. MFS transporters are currently the best characterised superfamily of secondary transmembrane transport proteins responsible for nutrient uptake, extrusion of metabolites and resistance to various toxic compounds, including not only secondary metabolites but also fungicides and antibiotics. On the other hand, MFS transporters play a role in the availability of nutrients for survival, including the transport of lipids, ions and small metabolites [57]. The transcript abundance of the MFS multidrug transporter was five times higher in pathogenic *F. oxysporum* than in non-pathogenic *F. oxysporum*. This transporter family regulates the movement of sugars, Krebs cycle metabolites, phosphorylated glycolytic intermediates, amino acids, peptides, osmoliths, iron siderophores, nucleosides, and organic and inorganic anions and cations [58]. In addition, MFS transporters have been linked to fungal pathogenicity by avoiding toxic compounds produced by the pathogen or protecting against plant defences [59]. On Chr12, not only the putative CTF gene but also putative genes encoding proteins containing lipase (*g71*, *g102*), COesterase (*g81*), peptidase (*g18* and *g89*) and domains of MFS (*g66* and *g105*) are localised.

Species of the genus *Fusarium* produce a wide variety of agriculturally important trichothecene toxins, which differ from each other in their pattern of oxygenation and esterification. Trichothecenes are a structurally diverse family of fungal sesquiterpene epoxides that cause mycotoxicosis in humans and animals and increase the virulence of some *Fusarium* species on crops. In *F. sporotrichioides* and *F. graminearum*, trichothecene biosynthetic genes are localised in a 40-kb gene cluster [60,61]. Genes in this cluster include trichodiene synthetase, P450 oxygenase, acetyltransferase, a toxin efflux pump

and transcription factors containing a Cys2His2 zinc finger motif [62]. On Chr12, genes involved in trichothecene synthesis were found - a putative tyrosinase gene (*g6*), acyl-CoA dehydrogenase (*g70*) and p450 cytochrome oxidase (*g95*), but not organised in a cluster.

The gene *g2* encodes a protein containing a GPI-anchored domain found at the N-terminus of a group of cell wall synthesis proteins involved in the synthesis of beta-1,6-glucan in the cell wall [63]. The cell wall shapes and protects the fungal cell. The 1,3-beta-glucan synthase is responsible for the synthesis of one of the main components of the fungal wall. This enzyme has been described in *F. solani* and many other *Fusarium* species [64]. Many attempts to delete the gene encoding this enzyme have been unsuccessful, suggesting that it may be a gene essential for cell life [65].

A comparison of the expression of serine/threonine protein kinase genes (*ste12*) in pathogenic and non-pathogenic strains of *F. oxysporum* f. sp. *cubense* showed a significant increase in the expression of *ste12* in pathogenic strains [66]. Deletion of *FgPTC1*, a serine/threonine phosphatase, also attenuated the virulence of *F. graminearum* on wheat [67]. The mutant of *F. verticillioides* in which the *fpk1* gene encoding the cAMP-dependent protein kinase was disrupted showed reduced vegetative growth, fewer and shorter aerial mycelia, severely impaired conidiation and reduced spore germination rate. After germination, the fresh hyphae were stout and unbranched. When inoculated into susceptible maize varieties, infection of the delta *fpk1* mutant was delayed and infection efficiency was reduced compared to the wild-type strain [68]. Family of serine/threonine protein kinases and plays an important role in yeasts and other filamentous fungi. Deletion of *FoIme2*, which belongs to this family, in *F. oxysporum* reduced mycelial growth and conidia production. The mutants were hypersensitive to the osmotic stressor NaCl but less sensitive to the membrane stressor SDS. Deletion of *FoIme2* also reduced pathogenicity [69]. The gene encoding the protein kinase (*g56*) is located on Chr 12.

In filamentous fungi, gene silencing by RNA interference (RNAi) affects many biological processes, including pathogenicity. Deletion of *qde3*, which encodes helicase, impaired conidiation and ascosporegenesis in *F. graminaceum* and contributes to sexual reproduction [70]. Chr. 12 contains the gene *g74*, which encodes a protein containing a helicase domain.

5. Conclusions

- Overall, the knowledge gained in this study about the annotations of genes, ORFs and domains in the 12th chromosome of *F. circinatum* could make an important contribution to the management of PPC disease and to strategies for containment and mitigation strategies.
- Our study can serve to clarify the phylogeny of the species and furthermore to develop new molecular detection tools.
- The genomic organisation of virulence genes can be used to clarify the relationship between *F. circinatum* and hosts.
- We concluded that at least 14 genes are associated with pathogenesis/virulence.

Author Contributions: Conceptualization, T.M., S.M., A.O.; methodology, T.M., S.M., A.O.; software, T.M., P.B.; validation, T.M., P.B.; formal analysis, T.M., P.B.; investigation, T.M.; resources, A.O., T.M.; data curation, P.B.; writing—original draft preparation, T.M., T.O.; writing—review and editing, T.O., P.B., S.M.; visualization, P.B., T.M.; supervision, T.M., T.O.; project administration, T.M., T.O.; funding acquisition, A.O. All authors have read and agreed to the published version of the manuscript.

Funding: The publication was written as a part of result of the author's (AO) internship in Slovak University of Agriculture in Nitra, co-financed by the European Union under the European Social Fund (Operational Program Knowledge Education Development), carried out in the project Development Program at the University of Warmia and Mazury in Olsztyn (POWR.03.05. 00-00-Z310/17).

Institutional Review Board Statement: Not applicable.

Informed Consent Statement: Not applicable.

Data Availability Statement: Not applicable.

Conflicts of Interest: The authors declare no conflict of interest.

Appendix A. Localization and Annotation of Putative *F. circinatum* Proteins

Table A1. Localization of putative Open Reading Frames and transcripts, protein sizes, and number of introns derived from the *F. circinatum* 12th chromosome annotation.

Gene	Strand	Localization	No. Introns	Transcript	Localization	Predicted Protein Size
1	+	31217–31960	2	1	31217–31219	196
	+		2	2	31229–31960	192
2	+	33294–34089	1		33294–34089	238
3	–	36737–36989	1		36737–36989	68
4	+	38485–39264	0		38485–39264	259
5	+	40947–41501	0		40947–41501	184
6	–	42288–44793	7	1	42288–44793	687
			7	2	42288–44793	687
7	+	47832–50343	3		47832–50343	712
8	+	50528–51772	0		50528–51772	414
9	–	53269–53616	0		53269–53616	115
10	–	53692–54501	0		53692–54501	269
11	–	58288–59517	1		58288–59517	393
12	–	67276–67674	0		67276–67674	132
13	–	69092–69550	0		69092–69550	152
14	–	71147–71430	0		71147–71430	75
15	+	71985–72521	1		71985–72521	136
16	–	76693–77699	1		76693–77699	300
17	+	81870–83876	0		81870–83876	668
18	–	83977–85827	0		83977–85827	618
19	–	87569–88259	2		87569–88259	194
20	+	89834–92287	0		89834–92287	817
21	+	95681–96392	1	1	95681–96392	219
	+		1	2	95777–96392	187
22	–	101909–103049	4	1	101973–103049	148
			5	2	101909–103049	195
23	+	104774–105565	2		104774–105565	223
24	+	108785–110371	0		108785–110371	528
25	+	115888–116535	2		115888–116535	146
26	–	117728–122084	2		117728–122084	1379
27	–	130442–131614	4		130442–131614	323
28	+	133748–134953	3	1	133982–134953	271
			6	2	133748–134953	297
29	–	138883–139227	0		138883–139227	114
30	–	143831–145637	5		143831–145637	441
31	+	145727–148851	11		145727–148851	475
32	+	156385–157122	1		156385–157122	228
33	–	157739–158284	0		157739–158284	181
34	–	165252–166541	0		165252–166541	429
35	–	167760–169128	2		167760–169128	311
36	+	171554–172271	1	1	171554–172271	178
			2		171578–172271	170
37	+	173661–174852	2		173661–174852	364
38	+	177631–179403	3		177631–179403	368
39	–	179756–180727	2	1	179756–180727	285
			2	2	179756–180727	288
40	+	180965–181919	1		180965–181919	209
41	–	181947–182603	2		181947–182603	185
42	–	184433–186403	3	1	184433–186403	436
			4	2	184433–186403	461
43	–	197699–198520	1		197699–198520	131
44	+	201599–202213	0		201599–202213	204
45	–	206352–206792	1		206352–206792	114
46	–	212670–213117	1		212670–213117	117
47	–	217694–218296	1		217694–218296	134
48	–	219886–220412	1		219886–220412	153

Table A1. Cont.

Gene	Strand	Localization	No. Introns	Transcript	Localization	Predicted Protein Size
49	+	241829–243064	4		241829–243064	292
50	+	249462–249912	1		249462–249912	132
51	—	255019–255430	1		255019–255430	117
52	—	260511–267687	4		260511–267687	1871
53	+	267833–269506	0		267833–269506	557
54	+	269924–270610	0		269924–270610	228
55	—	270814–272503	4	1	270814–272503	442
			4	2	270814–272503	433
56	—	279820–281924	2		279820–281924	636
57	+	284917–288900	5		284917–288900	1103
58	+	290740–294512	8	1	290740–294512	993
			8	2	290740–290742	1008
59	—	296603–298423	1		296603–298423	465
60	—	299021–300337	0		299021–300337	436
61	+	301149–301535	0		301149–301535	128
62	+	306378–309789	3		306378–309789	987
63	+	312081–313133	0		312081–313133	350
64	—	314421–314718	1		314421–314718	82
65	—	316363–317384	2		316363–317384	304
66	+	319615–321355	1	1	319636–321355	550
			1	2	319615–321355	557
67	—	321897–322763	0		321897–322763	288
68	+	324749–325970	3		324749–325970	339
69	+	327367–328119	0		327367–328119	250
70	—	328511–329701	0		328511–329701	396
71	—	333730–334527	0		333730–334527	165
72	—	335535–336444	1		335535–336444	141
73	+	339435–340126	1	1	339435–340042	186
			2	2	339435–340126	196
74	—	340698–341147	2		340698–341147	116
75	—	344219–347477	2		344219–347477	1042
76	+	349423–350519	2	1	349423–350519	331
			1	2	349423–350519	347
77	—	352248–352879	1		352248–352879	118
78	+	353875–354707	1		353875–354707	235
79	+	358678–362423	5		358678–362423	1046
80	—	364509–365599	1		364509–365599	346
81	—	368775–372232	5	1	368775–372232	660
			5	2	368775–372232	634
82	—	373134–374775	1		373134–374775	527
83	+	375893–377234	1		375893–377234	428
84	—	377746–379869	2		377746–379869	638
85	+	381383–382024	0		381383–382024	213
86	+	384422–387495	3	1	386043–387495	418
			0	2	384422–385309	295
			5	3	384422–387495	754
87	+	389607–393031	6	1	389607–393031	550
			7	2	389607–393031	531
88	+	393067–393411	0		393067–393411	114
89	+	396581–397378	1	1	396650–397378	167
			1	2	396581–397378	190
90	—	399885–401207	2		399885–401207	504
91	—	403346–403807	0		403346–403807	153
92	—	405413–405787	2	1	405413–405787	92
			1	2	405413–405738	91
93	—	412668–413939	1		412668–413939	407
94	+	418703–419415	2		418703–419415	201
95	—	419654–420268	0		419654–420268	204
96	—	423279–424095	2		423279–424095	240
97	—	432389–433183	0		432389–433183	264
98	—	437147–438263	1		437147–438263	327
99	—	441782–442974	1	1	441782–442974	379
			2	2	441782–442974	349
100	—	444928–446536	2		444928–446536	502
101	+	447456–448802	3		447456–448802	392
102	+	451345–452097	0		451345–452097	250

Table A1. Cont.

Gene	Strand	Localization	No. Introns	Transcript	Localization	Predicted Protein Size
103	+	459258–461038	2		459258–461038	552
104	+	462490–462897	1		462490–462897	102
105	—	465130–468729	9		465130–468729	888
106	+	476676–478090	1		476676–478090	448
107	—	481803–482006	0		481803–482006	67
108	—	486871–487349	1		486871–487349	141
109	—	490202–492772	4		490202–492772	528
110	+	490202–492772	1		490202–492772	156
111	+	497012–498151	0		497012–498151	379
112	+	499716–500198	0		499716–500198	160
113	—	502582–504360	1		502582–504360	508
114	+	506239–507444	3	1	506239–507444	174
			2	2	506239–507444	161
115	+	508757–509677	2	1	508757–509677	198
			3	2	508757–509677	239
116	+	511677–512903	0		511677–512903	408
117	—	513379–514311	2		513379–514311	137
118	+	515695–516607	1		515695–516607	249

Table A2. GenBank best matches of putative *F. circinatum* proteins.

Protein	Length (AA)	Best Match ID	Accession No. (Best Match)	E Value	Identity (%)
g1t1	196	Hypothetical protein FCIRC_1200 <i>F. circinatum</i>	KAF5689737.1	5×10^{-129}	100.00
g1t2	192	Hypothetical protein FCIRC_1200 <i>F. circinatum</i>	XP_049150203.1	4×10^{-129}	100.00
g2t1	238	Cell wall beta-glucan synthesis, FCIRC_1201, <i>F. circinatum</i>	KAF5689738.1	1×10^{-170}	100.00
g3t1	68	Hypothetical protein FCIRC_1202, <i>F. circinatum</i>	KAF5689739.1	3×10^{-40}	100.00
g4t1	258	Hypothetical protein, FCIRC_1203 <i>F. circinatum</i>	KAF5689740.1	0.0	100.00
g5t1	184	Hypothetical protein FCIRC_1204 <i>F. circinatum</i>	KAF5689741.1	9×10^{-135}	100.00
g6t1	687	Tyrosinase precursor, FCIRC_1205, <i>F. circinatum</i>	KAF5689742.1	0.0	100.00
g6t2	687	Tyrosinase precursor, FCIRC_1205, <i>F. circinatum</i>	KAF5689742.1	0.0	98.84
g7t1	712	Extracellular gdsl-like lipase, FCIRC_1206, <i>F. circinatum</i>	KAF5689743.1	0.0	100.00
g8t1	414	Hypothetical protein FCIRC_1207 <i>F. circinatum</i>	KAF5689744.1	0.0	100.00
g9t1	115	Hypothetical protein FCIRC_1208, <i>F. circinatum</i>	KAF5689745.1	1×10^{-75}	100.00
g10t1	269	Hypothetical protein FCIRC_1209, <i>F. circinatum</i>	KAF5689746.1	0.0	100.00
g11t1	393	Hypothetical protein FCIRC_1210, <i>F. circinatum</i>	KAF5689747.1	0.0	100.00
g12t1	132	Hypothetical protein FCIRC_1211, <i>F. circinatum</i>	KAF5689748.1	2×10^{-90}	100.00
g13t1	152	Hypothetical protein FCIRC_1212, <i>F. circinatum</i>	KAF5689749.1	2×10^{-107}	100.00
g14t1	75	Hypothetical protein FCIRC_1213, <i>F. circinatum</i>	KAF5689750.1	3×10^{-47}	100.00
g15t1	136	Hypothetical protein FCIRC_1214, <i>F. circinatum</i>	KAF5689751.1	1×10^{-94}	100.00
g16t1	300	Serine threonine kinase, FCIRC_1215, <i>F. circinatum</i>	KAF5689752.1	7×10^{-167}	81.33
g17t1	668	Hypothetical protein CIRC_1216, <i>F. circinatum</i>	KAF5689753.1	0.0	100.00
g18t1	616	Hypothetical protein CIRC_1217, <i>F. circinatum</i>	KAF5689754.1	0.0	100.00
g19t1	194	Hypothetical protein CIRC_1218, <i>F. circinatum</i>	KAF5689755.1	2×10^{-136}	100.00
g20t1	817	Transcription factor jumonji, FCIRC_1219, <i>F. circinatum</i>	KAF5689756.1	0.0	100.00
g21t1	219	Hypothetical protein CIRC_1220, <i>F. circinatum</i>	KAF5689757.1	6×10^{-154}	92.80
g21t2	187	Hypothetical protein FCIRC_1220, <i>F. circinatum</i>	KAF5689757.1	5×10^{-130}	91.67
g22t1	148	Hypothetical protein FCIRC_1222, <i>F. circinatum</i>	KAF5689759.1	2×10^{-88}	99.23
g22t2	195	Hypothetical protein FCIRC_1222, <i>F. circinatum</i>	KAF5228515.1	1×10^{-129}	93.33
g23t1	223	Hypothetical protein CIRC_1223, <i>F. circinatum</i>	KAF5689760.1	1×10^{-165}	100.00
g24t1	528	Hypothetical protein CIRC_1224, <i>F. circinatum</i>	KAF5689761.1	0.0	100.00
g25t1	146	Hypothetical protein CIRC_1225, <i>F. circinatum</i>	KAF5689762.1	5×10^{-102}	100.00
g26t1	1379	Ankyrin repeat protein, FCIRC_1226, <i>F. circinatum</i>	KAF5689763.1	0.0	100.00
g27t1	323	Hypothetical protein CIRC_1227, <i>F. circinatum</i>	KAF5689764.1	0.0	100.00

Table A2. Cont.

Protein	Length (AA)	Best Match ID	Accession No. (Best Match)	E Value	Identity (%)
g28t1	271	Hypothetical protein FCIRC_1228, <i>F. circinatum</i>	KAF5689765.1	0.0	100.00
g28t2	297	Hypothetical protein FCIRC_1228, <i>F. circinatum</i>	KAF5689765.1	0.0	100.00
g29t1	114	Hypothetical protein FCIRC_1229, <i>F. circinatum</i>	KAF5689766.1	3×10^{-77}	100.00
g30t1	441	Hypothetical protein FCIRC_1230, <i>F. circinatum</i>	KAF5689767.1	0.0	100.00
g31t1	475	Translation initiation factor IF-2, FCIRC_1231, <i>F. circinatum</i>	KAF5689768.1	4×10^{-179}	96.51
g32t1	228	Hypothetical protein FCIRC_1232, <i>F. circinatum</i>	KAF5689769.1	1×10^{-158}	100.00
g33t1	181	Hypothetical protein FCIRC_1233, <i>F. circinatum</i>	KAF5689770.1	2×10^{-131}	100.00
g34t1	429	Hypothetical protein FCIRC_1234, <i>F. circinatum</i>	KAF5689771.1	0.0	100.00
g35t1	311	C2H2 transcription factor, FCIRC_1235, <i>F. circinatum</i>	KAF5689772.1	0.0	100.00
g36t1	178	Hypothetical protein FCIRC_1237, <i>F. circinatum</i>	KAF5689774.1	1×10^{-126}	100.00
g36t2	170	Hypothetical protein FCIRC_1237, <i>F. circinatum</i>	KAF5689774.1	9×10^{-120}	100.00
g37t1	364	Hypothetical protein FCIRC_1729, <i>F. circinatum</i>	KAF5688719.1	0.0	100.00
g38t1	368	Hypothetical protein FCIRC_1731, <i>F. circinatum</i>	KAF5688721.1	0.0	100.00
g39t1	285	Hypothetical protein FCIRC_1732, <i>F. circinatum</i>	KAF5688722.1	0.0	100.00
g39t2	288	Hypothetical protein FCIRC_1732, <i>F. circinatum</i>	KAF5688722.1	0.0	98.61
g40t1	209	Hypothetical protein FCIRC_1733, <i>F. circinatum</i>	KAF5688723.1	1×10^{-150}	100.00
g41t1	185	Hypothetical protein FCIRC_1734, <i>F. circinatum</i>	KAF5688724.1	2×10^{-135}	100.00
g42t1	436	Hypothetical protein FCIRC_1735, <i>F. circinatum</i>	KAF5688725.1	0.0	99.74
g42t2	461	Hypothetical protein FCIRC_1735, <i>F. circinatum</i>	KAF5688725.1	0.0	99.74
g43t1	131	FK506-binding protein, FCIRC_1236, <i>F. circinatum</i>	KAF5688726.1	8×10^{-93}	100.00
g44t1	204	Hypothetical protein FCIRC_1737, <i>F. circinatum</i>	KAF5688727.1	2×10^{-144}	100.00
g45t1	114	Hypothetical protein FCIRC_1738, <i>F. circinatum</i>	KAF5688728.1	5×10^{-78}	100.00
g46t1	117	Hypothetical protein FCIRC_1739, <i>F. circinatum</i>	KAF5688729.1	7×10^{-77}	100.00
g47t1	134	Hypothetical protein FCIRC_1740, <i>F. circinatum</i>	KAF5688730.1	1×10^{-92}	100.00
g48t1	153	Arginine deiminase type-3, <i>F. mexicanum</i>	KAF5555127.1	1×10^{-95}	95.83
g49t1	292	Hypothetical protein FCIRC_10050, <i>F. circinatum</i>	KAF5666814.1	0.0	100.00
g50t1	132	Hypothetical protein FCIRC_10051, <i>F. circinatum</i>	KAF5666815.1	1×10^{-92}	100.00
g51t1	117	Sterol 3beta-glucosyltransferase, FCIRC_10052, <i>F. circinatum</i>	KAF5666816.1	2×10^{-60}	100.00
g52t1	1871	NACHT ankyrin domain-containing protein, FCIRC_10053, <i>F. circinatum</i>	KAF5666817.1	0.0	100.00
g53t1	557	NCS1 nucleoside transporter, FCIRC_10054, <i>F. circinatum</i>	KAF5666818.1	0.0	100.00
g54t1	228	Asp glu hydantoin racemase, FCIRC_10055, <i>F. circinatum</i>	KAF5666819.1	6×10^{-163}	100.00
g55t1	442	C6 transcription factor, FCIRC_10056, <i>F. circinatum</i>	KAF5666820.1	0.0	97.96
g55t2	433	C6 transcription factor, FCIRC_10056, <i>F. circinatum</i>	KAF5666820.1	0.0	100.00
g56t1	638	CMGC DYRK kinase, FCIRC_10058, <i>F. circinatum</i>	KAF5666822.1	0.0	100.00
g57t1	1103	Serine threonine kinase, FCIRC_10059, <i>F. circinatum</i>	KAF5666823.1	0.0	100.00
g58t1	993	NACHT domain-containing protein, FCIRC_5226, <i>F. circinatum</i>	KAF5682015.1	0.0	99.59
g58t2	1008	NACHT domain-containing protein, FCIRC_5226, <i>F. circinatum</i>	KAF5682015.1	0.0	92.73
g59t1	465	TPR domain-containing protein, <i>F. denticulatum</i>	KAF5674688.1	0.0	55.26
g60t1	438	TPR domain-containing protein, FCIRC_5228, <i>F. circinatum</i>	KAF5682016.1	0.0	100.00
g61t1	128	Hypothetical protein FCIRC_5229, <i>F. circinatum</i>	KAF5682017.1	2×10^{-88}	100.00
g62t1	987	Hypothetical protein FCIRC_5230, <i>F. circinatum</i>	KAF5682018.1	0.0	92.40
g63t1	350	Hypothetical protein FCIRC_5231, <i>F. circinatum</i>	KAF5682019.1	0.0	98.86
g64t1	82	Hypothetical protein FCIRC_5232, <i>F. circinatum</i>	KAF5682020.1	5×10^{-53}	100.00
g65t1	304	Aspartate aminotransferase, FCIRC_5233, <i>F. circinatum</i>	KAF5682021.1	1×10^{-136}	100.00
g66t1	550	Multidrug resistance protein fnx1, FCIRC_8030, <i>F. circinatum</i>	KAF5673567.1	0.0	100.00

Table A2. Cont.

Protein	Length (AA)	Best Match ID	Accession No. (Best Match)	E Value	Identity (%)
g66t2	557	Multidrug resistance protein fnx1, FCIRC_8030, <i>F. circinatum</i>	KAF5673567.1	0.0	100.00
g67t1	288	D-isomer specific 2-hydroxyacid dehydrogenase, FCIRC_8029, <i>F. circinatum</i>	KAF5673566.1	0.0	100.00
g68t1	339	Macrophomate synthase, FCIRC_8028, <i>F. circinatum</i>	KAF5673565.1	0.0	100.00
g69t1	250	Demethylmenaquinone methyltransferase family, FCIRC_8027, <i>F. circinatum</i>	KAF5673564.1	0.0	100.00
g70t1	396	Hypothetical protein FCIRC_8026, <i>F. circinatum</i>	KAF5673563.1	0.0	100.00
g71t1	165	Hypothetical protein FCIRC_8025, <i>F. circinatum</i>	KAF5673562.1	1×10^{-119}	100.00
g72t1	141	Hypothetical protein FCIRC_8024, <i>F. circinatum</i>	KAF5673561.1	2×10^{-98}	100.00
g73t1	186	Hypothetical protein FCIRC_8023, <i>F. circinatum</i>	KAF5673560.1	3×10^{-133}	100.00
g73t2	196	Hypothetical protein FCIRC_8023, <i>F. circinatum</i>	KAF5673560.1	4×10^{-124}	100.00
g74t1	116	SNF2 family domain containing protein, <i>F. agapanthi</i>	KAF4497424.1	6×10^{-65}	92.24
g75t1	1042	Hypothetical protein FCIRC_8022, <i>F. circinatum</i>	KAF5673559.1	0.0	100.00
g76t1	331	Hypothetical protein FCIRC_8021, <i>F. circinatum</i>	KAF5673558.1	0.0	100.00
g76t2	347	Hypothetical protein FCIRC_8021, <i>F. circinatum</i>	KAF5673558.1	0.0	95.39
g77t1	118	Hypothetical protein FCIRC_8020, <i>F. circinatum</i>	KAF5673557.1	5×10^{-82}	100.00
g78t1	235	Kinase-like domain-containing protein, FCIRC_8019, <i>F. circinatum</i>	KAF5673556.1	9×10^{-167}	87.97
g79t1	1046	Hypothetical protein FCIRC_8018, <i>F. circinatum</i>	KAF5673555.1	0.0	100.00
g80t1	346	Hypothetical protein FCIRC_8017, <i>F. circinatum</i>	KAF5673554.1	0.0	100.00
g81t1	660	Para-nitrobenzyl esterase, FCIRC_8016, <i>F. circinatum</i>	KAF5673553.1	0.0	100.00
g81t2	634	Para-nitrobenzyl esterase, FCIRC_8016, <i>F. circinatum</i>	KAF5673553.1	0.0	96.06
g82t1	527	Cutinase transcription factor 1 alpha, FCIRC_8015, <i>F. circinatum</i>	KAF5673552.1	0.0	100.00
g83t1	428	Hypothetical protein FCIRC_8014, <i>F. circinatum</i>	KAF5673551.1	0.0	100.00
g84t1	638	Hypothetical protein FCIRC_8013, <i>F. circinatum</i>	KAF5673550.1	0.0	100.00
g85t1	213	Hypothetical protein FCIRC_8012, <i>F. circinatum</i>	KAF5673549.1	0.0	100.00
g86t1	418	Hypothetical protein FCIRC_8010, <i>F. circinatum</i>	KAF5673547.1	0.0	100.00
g86t2	295	Hypothetical protein FCIRC_8011, <i>F. circinatum</i>	KAF5673548.1	0.0	97.97
g86t3	754	SGL domain-containing protein, <i>Fusarium</i> sp. LHS14.1	KAI8724150.1	2×10^{-95}	52.38
g87t1	550	ATP synthase F1, FCIRC_8009, <i>F. circinatum</i>	KAF5673546.1	0.0	91.65
g87t2	531	ATP synthase F1, FCIRC_8009, <i>F. circinatum</i>	KAF5673546.1	0.0	87.94
g88t1	114	Hypothetical protein FCIRC_8008, <i>F. circinatum</i>	KAF5673545.1	8×10^{-77}	100.00
g89t1	167	Caspase, FCIRC_8007, <i>F. circinatum</i>	KAF5673544.1	1×10^{-121}	100.00
g89t2	190	Caspase, FCIRC_8007, <i>F. circinatum</i>	KAF5673544.1	2×10^{-121}	100.00
g90t1	405	Hypothetical protein FCIRC_8006, <i>F. circinatum</i>	KAF5673543.1	0.0	100.00
g91t1	153	Hypothetical protein FCIRC_8005, <i>F. circinatum</i>	KAF5673542.1	1×10^{-105}	100.00
g92t1	92	Hypothetical protein FCIRC_8004, <i>F. circinatum</i>	KAF5673541.1	8×10^{-60}	100.00
g92t2	91	Hypothetical protein FCIRC_8004, <i>F. circinatum</i>	KAF5673541.1	3×10^{-46}	86.52
g93t1	407	Transaldolase, FCIRC_7317, <i>F. circinatum</i>	KAF5675701.1	0.0	100.00
g94t1	201	Aromatic prenyltransferase, FCIRC_7316, <i>F. circinatum</i>	KAF5675700.1	2×10^{-142}	100.00
g95t1	204	Cytochrome P450 monooxygenase, FCIRC_7315, <i>F. circinatum</i>	KAF5675699.1	2×10^{-150}	100.00
g96t1	240	Nonribosomal peptide synthase, FCIRC_7314, <i>F. circinatum</i>	KAF5675698.1	8×10^{-176}	100.00
g97t1	264	Hypothetical protein FCIRC_7313, <i>F. circinatum</i>	KAF5675697.1	0.0	100.00
g98t1	327	Uncharacterized protein FSUBG_13770, <i>F. subglutinans</i>	XP_036530762.1	7×10^{-158}	64.23
G99t1	379	Hypothetical protein FCIRC_7311, <i>F. circinatum</i>	KAF5675696.1	0.0	84.22
g99t2	349	Hypothetical protein FCIRC_7311, <i>F. circinatum</i>	KAF5675696.1	0.0	76.34
g100t1	502	Rhs repeat-associated core domain-containing protein, FCIRC_7310, <i>F. circinatum</i>	KAF5675695.1	0.0	100.00
g101t1	392	Hypothetical protein FCIRC_7309, <i>F. circinatum</i>	KAF5675694.1	0.0	100.00
g102t1	250	Esterase SGNH hydrolase-type subgroup, FCIRC_7308, <i>F. circinatum</i>	KAF5675693.1	0.0	100.00

Table A2. Cont.

Protein	Length (AA)	Best Match ID	Accession No. (Best Match)	E Value	Identity (%)
g103t1	552	SET domain-containing protein, FCIRC_7305, <i>F. circinatum</i>	KAF5675692.1	0.0	100.00
g104t1	102	Hypothetical protein FCIRC_7306, <i>F. circinatum</i>	KAF5675691.1	3×10^{-67}	100.00
g105t1	888	Major facilitator superfamily transporter, FCIRC_7305 <i>F. circinatum</i>	KAF5675690.1	0.0	100.00
g106t1	448	Hypothetical protein FCIRC_7304, <i>F. circinatum</i>	KAF5675689.1	0.0	95.12
g107t1	67	Hypothetical protein FCIRC_7303, <i>F. circinatum</i>	KAF5675688.1	4×10^{-39}	100.00
g108t1	141	Hypothetical protein FCIRC_7302, <i>F. circinatum</i>	KAF5675687.1	2×10^{-95}	100.00
g109t1	528	Polyketide synthase FCIRC_7301, <i>F. circinatum</i>	KAF5675686.1	0.0	100.00
g110t1	156	Taurine dioxygenase family FCIRC_7300, <i>F. circinatum</i>	KAF5675685.1	2×10^{-110}	100.00
g111t1	379	Hypothetical protein FCIRC_7299, <i>F. circinatum</i>	KAF5675684.1	0.0	100.00
g112t1	160	Hypothetical protein FCIRC_7298, <i>F. circinatum</i>	KAF5675683.1	6×10^{-116}	100.00
g113t1	508	Hypothetical protein FCIRC_7297, <i>F. circinatum</i>	KAF5675682.1	0.0	100.00
g114t1	174	Kinase-like (PK-like), FCIRC_7296 <i>F. circinatum</i>	KAF5675681.1	8×10^{-88}	100.00
g114t2	161	Kinase-like (PK-like), FCIRC_7296 <i>F. circinatum</i>	KAF5675681.1	7×10^{-88}	100.00
g115t1	198	Hypothetical protein FCIRC_7295, <i>F. circinatum</i>	KAF5675680.1	4×10^{-132}	81.17
g115t2	239	Hypothetical protein FCIRC_7295, <i>F. circinatum</i>	KAF5675680.1	5×10^{-178}	100.00
g116t1	408	Alpha beta-hydrolase, FCIRC_7294, <i>F. circinatum</i>	KAF5675679.1	0.0	100.00
g117t1	137	Hypothetical protein FCIRC_7293, <i>F. circinatum</i>	KAF5675678.1	8×10^{-96}	100.00
g118t1	249	Telomere-associated recQ-like helicase, FCIRC_7292, <i>F. circinatum</i>	KAF5675677.1	0.0	100.00

Table A3. Protein domains identified by InterPro scan and SMART in putative *F. circinatum* proteins.

Gene	Pfam Acc. No.	InterPro Acc. No.	Domain Name	Domain Abbreviation	Name	Localization (AA)	E Value
g2t1	PF10342	IPR018466	Kre9/KNH-like N-terminal Ig-like domain	GPI-anchored		29–123	2.6×10^{-17}
g6t1	PF00264	IPR002227	Tyrosinase copper-binding	Tyrosinase		60–358	5.9×10^{-39}
g6t2	PF00264	IPR002227	Tyrosinase copper-binding	Tyrosinase		60–359	5.9×10^{-39}
g7t1	PF13472	IPR013830	SGNH hydrolase-type esterase	Lipase_GDSL_2		174–343	2.8×10^{-12}
g18t1	PF00112	IPR000668	Peptidase C1A, papain C-terminal	Peptidase_C1		434–607	4.9×10^{-7}
g20t1	-	IPR003347	Jumonji	JmjC		339–498	2.04×10^{-5}
g26t1	PF01048	IPR000845	Nucleoside phosphorylase	PNP_UDP_1		42–358	7.5×10^{-12}
g26t1	PF05729	IPR000845	NACHT nucleoside triphosphatase	NACHT		407–589	7.4×10^{-7}
g26t1	-	IPR002110	Ankyrin repeat	ANK		15 rpt. from 854 to 1374	
g52t1	PF03171	IPR005123	Oxoglutarate/iron-dependent dioxygenase	2OG-FeII_Oxy		49–158	2.8×10^{-17}
g52t1	PF01048	IPR000845	Nucleoside phosphorylase	PNP_UDP_1		175–472	3.3×10^{-7}
g52t1	PF05729	IPR007111	NACHT nucleoside triphosphatase	NACHT		575–742	1×10^{-6}
g53t1	PF02133	IPR001248	Purine-cytosine permease	Transp_cyt_pur		30–487	2.3×10^{-86}
g54t1	PF01177	IPR015942	Asp/Glu/hydantoin racemase	Asp_Glu_race		42–219	4×10^{-10}
g55t1	PF04082	IPR007219	Transcription factor, fungi	Fungal_trans		131–318	6×10^{-6}
g55t1	-	IPR001138	Zn(2)-C6 fungal-type DNA-binding	GAL4		6–54	4.19×10^{-4}
g55t2	PF04082	IPR007219	Transcription factor, fungi	Fungal_trans		130–318	5.7×10^{-6}
g55t2	-	IPR001138	Zn(2)-C6 fungal-type DNA-binding	GAL4		6–54	4.19×10^{-4}
g56t1	-	IPR000719	Protein kinase	S_TKc		29–359	9.33×10^{-9}
g57t1	-	PR000719	Protein kinase	S_TKc		167–466	0.142
g57t1	PF06985	IPR010730	Heterokaryon incompatibility	HET		693–821	5.4×10^{-7}
g58t1	PF05729	IPR007111	NACHT nucleoside triphosphatase	NACHT		291–469	9.7×10^{-8}
g58t1	-	IPR002110	Ankyrin repeats	ANK		6 rpt. from 711 to 963	
g58t2	PF05729	IPR007111	NACHT nucleoside triphosphatase	NACHT		291–469	9.9×10^{-8}
g58t2	-	IPR002110	Ankyrin repeats	ANK		6 rpt. from 726 to 978	
p65t1	PF00155	IPR004839	Aminotransferase, class I/class II	Aminotran_1_2		27–208	1.8×10^{-25}
p66t1	PF07690	IPR011701	Major facilitator superfamily	MSF1		61–459	2×10^{-45}

Table A3. Cont.

Gene	Pfam Acc. No.	InterPro Acc. No.	Domain Name	Domain Abbreviation	Name	Localization (AA)	E Value
p66t2	PF07690	IPR011701	Major facilitator superfamily	MSF1		86–466	2.1×10^{-45}
p67t1	PF02826	IPR006140	D-isomer specific 2-hydroxyacid dehydrogenase	2-Hacid_dh_C		60–256	1.1×10^{-46}
p68t1	PF03328	IPR005000	HpcH/HpaI aldolase/citrate lyase	HpcH_HpaI		37–257	5.9×10^{-25}
g70t1	PF02771	IPR013786	Acyl-CoA dehydrogenase/oxidase, N-terminal	Acyl-CoA_dh_N		5–117	9.2×10^{-18}
g70t1	PF02770	IPR006091	Acyl-CoA dehydrogenase/oxidase, middle	Acyl-CoA_dh_M		121–222	6.9×10^{-18}
g70t1	PF00441	IPR009075	Acyl-CoA dehydrogenase/oxidase, C-terminal	Acyl-CoA		234–390	2.7×10^{-32}
g74t1	PF00271	IPR001650	Helicase, C-terminal	helicase_C		14–116	1.8×10^{-8}
g79t1	-	IPR002110	Ankyrin repeats	ANK		9 rpt. from 275 to 275	
g81t1	PF00135	IPR00201	Carboxylesterase, type B	COesterase		33–488	1.1×10^{-93}
g81t2	PF00135	IPR00201	Carboxylesterase, type B	COesterase		33–364	4.9×10^{-83}
g82t1	-	IPR007219	Transcription factor, fungi	Fungal_trans		242–314	1.16×10^{-6}
g89t1	PF00656	IPR011600	Peptidase C14, caspase	Caspase		40–158	7×10^{-9}
g89t2	PF00656	IPR011600	Peptidase C14, caspase	Caspase		63–181	1×10^{-8}
g93t1	PF03702	IPR005338	Anhydro-N-acetylmuramic acid kinase	AnmK		2–382	1.9×10^{-60}
g94t1	PF11991	IPR017795	Aromatic prenyltransferase, DMATS-type	Trp_DMAT		1–193	1.1×10^{-27}
g95t1	PF00067	IPR001128	Cytochrome P450	p450		24–182	6.1×10^{-15}
g96t1	PF00501	IPR000873	AMP-dependent synthetase/ligase	AMP-binding		4–83	9.5×10^{-8}
g100t1	PF03534	IPR003284	Salmonella virulence plasmid protein	SpvB		47–240	1.1×10^{-51}
g102t1	PF13472	IPR013830	SGNH hydrolase-type esterase	Lipase_GDSL_2		22–239	1.5×10^{-11}
g103t1	-	IPR001214	SET domain	SET		7–155	8.47×10^{-12}
g105t1	PF07690	IPR011701	Major facilitator superfamily	MSF1		38–416	3.5×10^{-38}
g109t1	PF00109	IPR014030	Beta-ketoacyl synthase, N-terminal	Ketoacyl-synt		1–76	3.2×10^{-10}
g109t1	PF00109	IPR014030	Beta-ketoacyl synthase, N-terminal	Ketoacyl-synt		72–166	4.2×10^{-23}
g109t1	PF02801	IPR014031	Beta-ketoacyl synthase, C-terminal	Ketoacyl-synt_C		174–274	5.3×10^{-22}

Table A4. Putative proteins of *F. circinatum* annotated by eggNOG.

Gene	eggNOG	Description
g9t1	arCOG00379	trimeric autotransporter adhesin
g10t1	7KF05	fibrous sheath CABYR-binding protein
g24t1	BKZCK	ZnF_C2H2
g27t1	5K2KN	sjoegren syndrome nuclear autoantigen 1
g47t1	5J4GB	anthrone oxygenases
g48t1	KOG1724	S-phase kinase-associated protein 1
g59t1	KOG4626	protein O-GlcNAc transferase
g60t1	KOG4626	protein O-GlcNAc transferase
g75t1	KOG1546	nicotinamide-nucleotide amidase
g81t1	7NBP8	abhydrolase_1 alpha/beta hydrolase
g81t2	7NBP8	abhydrolase_1 alpha/beta hydrolase
g101t1	7K74H	cupin domain

References

1. Aoki, T.; O'Donnell, K.; Geiser, D.M. Systematics of key phytopathogenic *Fusarium* species: Current status and future challenges. *J. Gen. Plant Pathol.* **2014**, *80*, 189–201. [[CrossRef](#)]
2. Dean, R.; Van Kan, J.A.; Pretorius, Z.A.; Hammond-Kosack, K.E.; Di Pietro, A.; Spanu, P.D.; Rudd, J.J.; Dickman, M.; Kahmann, R.; Ellis, J.; et al. The Top 10 fungal pathogens in molecular plant pathology. *Mol. Plant Pathol.* **2012**, *13*, 414–430. [[CrossRef](#)] [[PubMed](#)]

3. Martín-García, J.; Paraschiv, M.; Flores-Pacheco, J.A.; Chira, D.; Diez, J.J.; Fernández, M. Susceptibility of several northeastern conifers to *Fusarium circinatum* and strategies for biocontrol. *Forests* **2017**, *8*, 318. [[CrossRef](#)]
4. Wingfield, M.; Hammerbacher, A.; Ganley, R.; Steenkamp, E.; Gordon, T.; Wingfield, B.; Coutinho, T. Pitch canker caused by *Fusarium circinatum*—A growing threat to pine plantations and forests worldwide. *Australas. Plant Pathol.* **2008**, *37*, 319–334. [[CrossRef](#)]
5. Bezos, D.; Martinez-Alvarez, P.; Fernandez, M.; Diez, J.J. Epidemiology and management of pine pitch canker disease in Europe—A review. *Balt. For.* **2017**, *23*, 279–293.
6. Wingfield, B.D.; Steenkamp, E.T.; Santana, Q.C.; Coetzee, M.P.; Bam, S.; Barnes, I.; Beukes, C.W.; Chan, W.Y.; Vos, L.D.; Fourie, G.; et al. First fungal genome sequence from Africa: A preliminary analysis. *S. Afr. J. Sci.* **2012**, *108*, 1–9. [[CrossRef](#)]
7. Vos, L.D.; van der Nest, M.A.; van der Merwe, N.A.; Myburg, A.A.; Wingfield, M.J.; Wingfield, B.D. Genetic analysis of growth, morphology and pathogenicity in the F1 progeny of an interspecific cross between *Fusarium circinatum* and *Fusarium subglutinans*. *Fungal Biol.* **2011**, *115*, 902–908. [[CrossRef](#)]
8. Van Wyk, S.; Wingfield, B.D.; De Vos, L.; Santana, Q.C.; Van der Merwe, N.A.; Steenkamp, E.T. Multiple independent origins for a subtelomeric locus associated with growth rate in *Fusarium circinatum*. *IMA Fungus* **2018**, *9*, 27–36. [[CrossRef](#)]
9. Muñoz-Adalia, E.J.; Fernández, M.; Wingfield, B.D.; Diez, J.J. In silico annotation of five candidate genes associated with pathogenicity in *Fusarium circinatum*. *For. Pathol.* **2018**, *48*, e12417. [[CrossRef](#)]
10. Phasha, M.; Wingfield, M.; Wingfield, B.; Coetzee, M.; Hallen-Adams, H.; Fru, F.; Swalarsk-Parry, B.; Yilmaz, N.; Duong, T.; Steenkamp, E. *Ras2* is important for growth and pathogenicity in *Fusarium circinatum*. *Fungal Genet. Biol.* **2021**, *150*, 103541. [[CrossRef](#)]
11. Maphosa, M.N.; Steenkamp, E.T.; Kanzi, A.M.; Van Wyk, S.; De Vos, L.; Santana, Q.C.; Duong, T.A.; Wingfield, B.D. Intra-species genomic variation in the pine pathogen *Fusarium circinatum*. *J. Fungi* **2022**, *8*, 657. [[CrossRef](#)]
12. der Nest, M.V.; Olson, Å.; Lind, M.; Véllez, H.; Dalman, K.; Durling, M.B.; Karlsson, M.; Stenlid, J. Distribution and evolution of *het* gene homologs in the basidiomycota. *Fungal Genet. Biol.* **2014**, *64*, 45–57. [[CrossRef](#)] [[PubMed](#)]
13. Stanke, M.; Morgenstern, B. AUGUSTUS: A web server for gene prediction in eukaryotes that allows user-defined constraints. *Nucleic Acids Res.* **2005**, *33*, W465–W467. [[CrossRef](#)] [[PubMed](#)]
14. Hoff, K.J.; Stanke, M. WebAUGUSTUS—A web service for training AUGUSTUS and predicting genes in eukaryotes. *Nucleic Acids Res.* **2013**, *41*, W123–W128. [[CrossRef](#)]
15. InterProScan. Available online: <https://www.ebi.ac.uk/interpro/search/sequence/> (accessed on 15 January 2023).
16. Jones, P.; Binns, D.; Chang, H.Y.; Fraser, M.; Li, W.; McAnulla, C.; McWilliam, H.; Maslen, J.; Mitchell, A.; Nuka, G.; et al. InterProScan 5: Genome-scale protein function classification. *Bioinformatics* **2014**, *30*, 1236–1240. [[CrossRef](#)]
17. Blum, M.; Chang, H.Y.; Chuguransky, S.; Grego, T.; Kandasamy, S.; Mitchell, A.; Nuka, G.; Paysan-Lafosse, T.; Qureshi, M.; Raj, S.; et al. The InterPro protein families and domains database: 20 years on. *Nucleic Acids Res.* **2020**, *49*, D344–D354. [[CrossRef](#)]
18. Letunic, I.; Khedkar, S.; Bork, P. SMART: Recent updates, new developments and status in 2020. *Nucleic Acids Res.* **2020**, *49*, D458–D460. [[CrossRef](#)]
19. Hernández-Plaza, A.; Szklarczyk, D.; Botas, J.; Cantalapiedra, C.P.; Giner-Lamia, J.; Mende, D.R.; Kirsch, R.; Rattei, T.; Letunic, I.; Jensen, L.J.; et al. eggNOG 6.0: Enabling comparative genomics across 12 535 organisms. *Nucleic Acids Res.* **2022**, *51*, D389–D394. [[CrossRef](#)] [[PubMed](#)]
20. Drenkhan, R.; Ganley, B.; Martín-García, J.; Vahalík, P.; Adamson, K.; Adamčíková, K.; Ahumada, R.; Blank, L.; Bragança, H.; Capretti, P.; et al. Global geographic distribution and host range of *Fusarium circinatum*, the causal agent of pine pitch canker. *Forests* **2020**, *11*, 724. [[CrossRef](#)]
21. Zamora-Ballesteros, C.; Diez, J.J.; Martín-García, J.; Witzell, J.; Solla, A.; Ahumada, R.; Capretti, P.; Cleary, M.; Drenkhan, R.; Dvořák, M.; et al. Pine pitch canker (PPC): Pathways of pathogen spread and preventive measures. *Forests* **2019**, *10*, 1158. [[CrossRef](#)]
22. Vainio, E.J.; Bezos, D.; Bragança, H.; Cleary, M.; Fourie, G.; Georgieva, M.; Ghelardini, L.; Hannunen, S.; Ioos, R.; Martín-Garcí, J.; et al. Sampling and detection strategies for the pine pitch canker (PPC) disease pathogen *Fusarium circinatum* in Europe. *Forests* **2019**, *10*, 723. [[CrossRef](#)]
23. Davydenko, K.; Nowakowska, J.A.; Kaluski, T.; Gawlik, M.; Sadowska, K.; García, J.M.; Diez, J.J.; Okorski, A.; Oszako, T. A Comparative Study of the Pathogenicity of *Fusarium circinatum* and other *Fusarium* Species in Polish Provenances of *P. sylvestris* L. *Forests* **2018**, *9*, 560. [[CrossRef](#)]
24. Raitelaitytė, K.; Oszako, T.; Markovskaja, S.; Radzijevskaja, J.; Paulauskas, A. *Fusarium circinatum* research on *Pinus sylvestris* of different provenances and interaction with other pine-inhabiting fungi. In Proceedings of the Smart Bio: ICSB 2nd International Conference, Kaunas, Lithuania, 3–5 May 2018; Vytautas Magnus University: Kaunas, Lithuania, 2018.
25. Elvira-Recuenco, M.; Cacciola, S.O.; Sanz-Ros, A.V.; Garbelotto, M.; Aguayo, J.; Solla, A.; Mullett, M.; Drenkhan, T.; Oskay, F.; Kaya, A.G.A.; et al. Potential interactions between invasive *Fusarium circinatum* and other pine pathogens in Europe. *Forests* **2019**, *11*, 7. [[CrossRef](#)]
26. Xu, J.R.; Yan, K.; Dickman, M.B.; Leslie, J.F. Electrophoretic karyotypes distinguish the biological species of *Gibberella fujikuroi* (*Fusarium section Liseola*). *MPMI-Mol. Plant Microbe Interact.* **1995**, *8*, 74–84. [[CrossRef](#)]
27. Saupe, S.J. Molecular Genetics of Heterokaryon Incompatibility in Filamentous Ascomycetes. *Microbiol. Mol. Biol. Rev.* **2000**, *64*, 489–502. [[CrossRef](#)] [[PubMed](#)]

28. Puhalla, J.E.; Spieth, P.T. A comparison of heterokaryosis and vegetative incompatibility among varieties of *Gibberella fujikuroi* (*Fusarium moniliforme*). *Exp. Mycol.* **1985**, *9*, 39–47. [CrossRef]
29. Paoletti, M.; Clavé, C. The Fungus-Specific HET Domain Mediates Programmed Cell Death in *Podospora anserina*. *Eukaryot. Cell* **2007**, *6*, 2001–2008. [CrossRef] [PubMed]
30. Dyrka, W.; Lamacchia, M.; Durrens, P.; Kobe, B.; Daskalov, A.; Paoletti, M.; Sherman, D.J.; Saupe, S.J. Diversity and Variability of NOD-Like Receptors in Fungi. *Genome Biol. Evol.* **2014**, *6*, 3137–3158. [CrossRef] [PubMed]
31. Saupe, S.; Turcq, B.; Bégueret, J. A gene responsible for vegetative incompatibility in the fungus *Podospora anserina* encodes a protein with a GTP-binding motif and G β homologous domain. *Gene* **1995**, *162*, 135–139. [CrossRef] [PubMed]
32. Koonin, E.V.; Aravind, L. The NACHT family—a new group of predicted NTPases implicated in apoptosis and MHC transcription activation. *Trends Biochem. Sci.* **2000**, *25*, 223–224. [CrossRef]
33. Bidard, F.; Clavé, C.; Saupe, S.J. The Transcriptional Response to Nonself in the Fungus *Podospora anserina*. *G3 Genes Genomes Genet.* **2013**, *3*, 1015–1030. [CrossRef]
34. Shelest, E. Transcription Factors in Fungi: TFome Dynamics, Three Major Families, and Dual-Specificity TFs. *Front. Genet.* **2017**, *8*, 53. [CrossRef] [PubMed]
35. Chang, P.K.; Ehrlich, K.C. Genome-wide analysis of the Zn(II)2Cys6 zinc cluster-encoding gene family in *Aspergillus flavus*. *Appl. Microbiol. Biotechnol.* **2013**, *97*, 4289–4300. [CrossRef]
36. Galhano, R.; Illana, A.; Ryder, L.S.; Rodríguez-Romero, J.; Demuez, M.; Badaruddin, M.; Martinez-Rocha, A.L.; Soanes, D.M.; Studholme, D.J.; Talbot, N.J.; et al. Tpc1 is an important Zn(II)2Cys6 transcriptional regulator required for polarized growth and virulence in the rice blast fungus. *PLoS Pathog.* **2017**, *13*, e1006516. [CrossRef] [PubMed]
37. Hou, Z.; Chen, Q.; Zhao, M.; Huang, C.; Wu, X. Genome-wide characterization of the Zn(II)2Cys6 zinc cluster-encoding gene family in *Pleurotus ostreatus* and expression analyses of this family during developmental stages and under heat stress. *PeerJ* **2020**, *8*, e9336. [CrossRef] [PubMed]
38. Niño-Sánchez, J.; Castillo, V.C.D.; Tello, V.; Vega-Bartol, J.J.D.; Ramos, B.; Sukno, S.A.; Minguez, J.M.D. The FTF gene family regulates virulence and expression of SIX effectors in *Fusarium oxysporum*. *Mol. Plant Pathol.* **2016**, *17*, 1124–1139. [CrossRef]
39. Mahanty, B.; Mishra, R.; Joshi, R.K. Molecular characterization of Zn(II)2Cys6 cluster gene family and their association with pathogenicity of the onion basal rot pathogen, *Fusarium oxysporum* f. sp. *cepae*. *Physiol. Mol. Plant Pathol.* **2022**, *117*, 101782. [CrossRef]
40. Li, D.; Sirakova, T.; Rogers, L.; Ettinger, W.F.; Kolattukudy, P. Regulation of constitutively expressed and induced cutinase genes by different zinc finger transcription factors in *Fusarium solani* f. sp. *pisi* (nectria haematococca). *J. Biol. Chem.* **2002**, *277*, 7905–7912. [CrossRef]
41. Hynes, M.J.; Murray, S.L.; Duncan, A.; Khew, G.S.; Davis, M.A. Regulatory genes controlling fatty acid catabolism and peroxisomal functions in the filamentous fungus *Aspergillus nidulans*. *Eukaryot. Cell* **2006**, *5*, 794–805. [CrossRef]
42. Rocha, A.L.M.; Pietro, A.D.; Ruiz-Roldán, C.; Roncero, M.I.G. Ctf1, a transcriptional activator of cutinase and lipase genes in *Fusarium oxysporum* is dispensable for virulence. *Mol. Plant Pathol.* **2008**, *9*, 293–304. [CrossRef]
43. Gacek, A.; Strauss, J. The chromatin code of fungal secondary metabolite gene clusters. *Appl. Microbiol. Biotechnol.* **2012**, *95*, 1389–1404. [CrossRef] [PubMed]
44. Wagner, E.J.; Carpenter, P.B. Understanding the language of Lys36 methylation at histone H3. *Nat. Rev. Mol. Cell Biol.* **2012**, *13*, 115–126. [CrossRef] [PubMed]
45. Connolly, L.R.; Smith, K.M.; Freitag, M. The *Fusarium graminearum* histone H3 K27 methyltransferase KMT6 regulates development and expression of secondary metabolite gene clusters. *PLoS Genet.* **2013**, *9*, e1003916. [CrossRef]
46. Janevska, S.; Baumann, L.; Sieber, C.M.; Münsterkötter, M.; Ulrich, J.; Kämper, J.; Güldener, U.; Tudzynski, B. Elucidation of the two H3K36me3 histone methyltransferases Set2 and Ash1 in *Fusarium fujikuroi* unravels their different chromosomal targets and a major impact of Ash1 on genome stability. *Genetics* **2018**, *208*, 153–171. [CrossRef]
47. Lee, J.H.; Skalnik, D.G. CpG-binding protein (CXXC finger protein 1) is a component of the mammalian Set1 histone H3-Lys4 methyltransferase complex, the analogue of the yeast Set1/COMPASS complex. *J. Biol. Chem.* **2005**, *280*, 41725–41731. [CrossRef] [PubMed]
48. Freitag, M. Histone methylation by SET domain proteins in fungi. *Annu. Rev. Microbiol.* **2017**, *71*, 413–439. [CrossRef]
49. Gacek-Matthews, A.; Berger, H.; Sasaki, T.; Wittstein, K.; Gruber, C.; Lewis, Z.A.; Strauss, J. KdmB, a Jumonji histone H3 demethylase, regulates genome-wide H3K4 trimethylation and is required for normal induction of secondary metabolism in *Aspergillus nidulans*. *PLoS Genet.* **2016**, *12*, e1006222. [CrossRef]
50. Ma, L.J.; Geiser, D.M.; Proctor, R.H.; Rooney, A.P.; O'Donnell, K.; Trail, F.; Gardiner, D.M.; Manners, J.M.; Kazan, K. *Fusarium pathogenomics*. *Annu. Rev. Microbiol.* **2013**, *67*, 399–416. [CrossRef]
51. van Dam, P.; Fokkens, L.; Ayukawa, Y.; van der Gragt, M.; Ter Horst, A.; Brankovics, B.; Houterman, P.M.; Arie, T.; Rep, M. A mobile pathogenicity chromosome in *Fusarium oxysporum* for infection of multiple cucurbit species. *Sci. Rep.* **2017**, *7*, 9042. [CrossRef]
52. Voigt, C.A.; Schäfer, W.; Salomon, S. A secreted lipase of *Fusarium graminearum* is a virulence factor required for infection of cereals. *Plant J.* **2005**, *42*, 364–375. [CrossRef]

53. Nguyen, L.N.; Bormann, J.; Le, G.T.T.; Stärkel, C.; Olsson, S.; Nosanchuk, J.D.; Giese, H.; Schäfer, W. Autophagy-related lipase FgATG15 of *Fusarium graminearum* is important for lipid turnover and plant infection. *Fungal Genet. Biol.* **2011**, *48*, 217–224. [[CrossRef](#)]
54. Bravo-Ruiz, G.; Ruiz-Roldán, C.; Roncero, M.I.G. Lipolytic system of the tomato pathogen *Fusarium oxysporum* f. sp. *lycopersici*. *Mol.-Plant-Microbe Interact.* **2013**, *26*, 1054–1067. [[CrossRef](#)]
55. Jashni, M.K.; Dols, I.H.M.; Iida, Y.; Boeren, S.; Beenen, H.G.; Mehrabi, R.; Collemare, J.; de Wit, P.J.G.M. Synergistic action of a metalloprotease and a serine protease from *Fusarium oxysporum* f. sp. *lycopersici* cleaves chitin-binding tomato chitinases, reduces their antifungal activity, and enhances fungal virulence. *Mol.-Plant-Microbe Interact.* **2015**, *28*, 996–1008. [[CrossRef](#)]
56. Qian, H.; Song, L.; Wang, L.; Wang, B.; Liang, W. The secreted FoAPY1 peptidase promotes *Fusarium oxysporum* invasion. *Front. Microbiol.* **2022**, *13*, 1040302. [[CrossRef](#)]
57. Yan, N. Structural advances for the major facilitator superfamily (MFS) transporters. *Trends Biochem. Sci.* **2013**, *38*, 151–159. [[CrossRef](#)]
58. Stergiopoulos, I.; Zwiers, L.H.; Waard, M.A.D. Secretion of Natural and Synthetic Toxic Compounds from Filamentous Fungi by Membrane Transporters of the ATP-binding Cassette and Major Facilitator Superfamily. *Eur. J. Plant Pathol.* **2002**, *108*, 719–734. [[CrossRef](#)]
59. Sorbo, G.D.; jan Schoonbeek, H.; Waard, M.A.D. Fungal Transporters Involved in Efflux of Natural Toxic Compounds and Fungicides. *Fungal Genet. Biol.* **2000**, *30*, 1–15. [[CrossRef](#)]
60. Brown, D.W.; McCormick, S.P.; Alexander, N.J.; Proctor, R.H.; Desjardins, A.E. A Genetic and Biochemical Approach to Study Trichothecene Diversity in *Fusarium sporotrichioides* and *Fusarium graminearum*. *Fungal Genet. Biol.* **2001**, *32*, 121–133. [[CrossRef](#)]
61. Kimura, M.; Tokai, T.; O'Donnell, K.; Ward, T.J.; Fujimura, M.; Hamamoto, H.; Shibata, T.; Yamaguchi, I. The trichothecene biosynthesis gene cluster of *Fusarium graminearum* F15 contains a limited number of essential pathway genes and expressed non-essential genes. *FEBS Lett.* **2003**, *539*, 105–110. [[CrossRef](#)]
62. Hohn, T.M.; Krishna, R.; Proctor, R.H. Characterization of a Transcriptional Activator Controlling Trichothecene Toxin Biosynthesis. *Fungal Genet. Biol.* **1999**, *26*, 224–235. [[CrossRef](#)]
63. Costachel, C.; Coddeville, B.; Latgé, J.P.; Fontaine, T. Glycosylphosphatidylinositol-anchored fungal polysaccharide in *Aspergillus fumigatus*. *J. Biol. Chem.* **2005**, *280*, 39835–39842. [[CrossRef](#)]
64. Ruiz-Herrera, J.; Ortiz-Castellanos, L. Cell wall glucans of fungi. A review. *Cell Surf.* **2019**, *5*, 100022. [[CrossRef](#)]
65. Ha, Y.S.; Covert, S.F.; Momany, M. FsFKS1, the 1,3-β-Glucan Synthase from the Caspofungin-Resistant Fungus *Fusarium solani*. *Eukaryot. Cell* **2006**, *5*, 1036–1042. [[CrossRef](#)]
66. Sutherland, R.; Viljoen, A.; Myburg, A.A.; den Berg, N.V. Pathogenicity associated genes in *Fusarium oxysporum* f. sp. *cubense* race 4. *S. Afr. J. Sci.* **2013**, *109*, 10. [[CrossRef](#)]
67. Jiang, L.; Yang, J.; Fan, F.; Zhang, D.; Wang, X. The Type 2C protein phosphatase FgPtc1p of the plant fungal pathogen *Fusarium graminearum* is involved in lithium toxicity and virulence. *Mol. Plant Pathol.* **2010**, *11*, 277–282. [[CrossRef](#)]
68. Pei-Bao, Z.; Ren, A.Z.; Xu, H.J.; Li, D.C. The gene *fpk1*, encoding a cAMP-dependent protein kinase catalytic subunit homolog, is required for hyphal growth, spore germination, and plant infection in *Fusarium verticillioides*. *J. Microbiol. Biotechnol.* **2010**, *20*, 208–216. [[CrossRef](#)]
69. Xiao, J.; Zhang, Y.; Yang, K.; Tang, Y.; Wei, L.; Liu, E.; Liang, Z. Protein kinase Ime2 is associated with mycelial growth, conidiation, osmoregulation, and pathogenicity in *Fusarium oxysporum*. *Arch. Microbiol.* **2022**, *204*. [[CrossRef](#)]
70. Gaffar, F.Y.; Imani, J.; Karlovsky, P.; Koch, A.; Kogel, K.H. Different Components of the RNA Interference Machinery Are Required for Conidiation, Ascosporegenesis, Virulence, Deoxynivalenol Production, and Fungal Inhibition by Exogenous Double-Stranded RNA in the Head Blight Pathogen *Fusarium graminearum*. *Front. Microbiol.* **2019**, *10*, 1662. [[CrossRef](#)]

Disclaimer/Publisher's Note: The statements, opinions and data contained in all publications are solely those of the individual author(s) and contributor(s) and not of MDPI and/or the editor(s). MDPI and/or the editor(s) disclaim responsibility for any injury to people or property resulting from any ideas, methods, instructions or products referred to in the content.